Supplementary material for:

Direct Conversion of Methane to Value-added Hydrocarbons Using Hybrid Catalysts of Ni/Al_2O_3 and $K\text{-}Co/Al_2O_3$

*Thitiwut Sukprom[1], Pooripong Somchuea[1], Sarannuch Sringam[1,2], Thongthai Witoon[1,2], Metta Chareonpanich[1,2], Pawin Iamprasertkun[3], Kajornsak Faungnawakij[4], Günther Rupprechter[5], Anusorn Seubsai[1,2]**

[1] *Department of Chemical Engineering, Faculty of Engineering, Kasetsart University, Bangkok 10900, Thailand*

[2] *Center of Excellence on Petrochemical and Materials Technology, Kasetsart University, Bangkok 10900, Thailand*

[3] *School of Bio-Chemical Engineering and Technology, Sirindhorn International Institute of Technology, Thammasat University, Pathum Thani, Thailand*

[4] *Nanomaterials for Energy and Catalysis Laboratory, National Nanotechnology Center (NANOTEC), National Science and Technology Development Agency (NSTDA), Pathum Thani 12120, Thailand*

[5] *Institute of Materials Chemistry, Technische Universität Wien, Getreidemarkt 9/BC, Vienna, 1060, Austria*

***Corresponding author**: fengasn@ku.ac.th

Methodology for making standard calibration curves

1) Premixed standard gases—containing CH_4, C_2H_4, C_2H_6, C_3H_6, C_3H_8, n-C_4H_{10}, iso-C_4H_{10}, CO, and CO_2—in a gas cylinder at 15 bars and ultra-high purity H_2 (99.999% purity) in a gas cylinder at 165 bars were purchased from Air LIQUID (Thailand) (see Table S1).
2) The premixed standard gases and H_2 were transferred to a gas sampling bag.
3) Five different volumes of the premixed standard gases and H_2 were injected into the gas chromatography (GC) using a gas syringe. The amount of the premixed gases and H_2 are shown in Table S1. The GC conditions are described in section "2.2 Catalytic activity test" of the main article.
4) Each GC peak from the flame ionization detector (FID) and thermal conductivity detector (TCD) signals was identified by comparing it with the known peaks from the "System Gas Chromatography (GC) Data Sheet" by Shimadzu or similar. Examples of GC chromatograms (both TCD and FID signals) of the standard gases and the effluents from the reaction are shown in Fig. S1–S4.
5) The GC peaks of each product were plotted with the moles that were obtained from the conversion of that gas volumes. Then, a calibration curve was made from the five spots on the plot, starting from the origin. The calibration curve of each standard gas is shown in Fig. S5–S14.

Table S1. Information on standard gases for making calibration curves

Standard gas	Concentration (% v/v)	Volume for GC injection
CH_4	5.00	0, 0.4, 0.5, 0.8, 1.0 mL
CO	5.01	
CO_2	4.99	
C_2H_4	4.97	0, 0.2, 0.4, 0.6, 0.8 mL
C_2H_6	5.03	
C_3H_6	5.03	
C_3H_8	5.00	
n-C_4H_{10}	5.02	
iso-C_4H_{10}	5.02	
H_2	99.999	0, 50, 100, 150, 200 µL

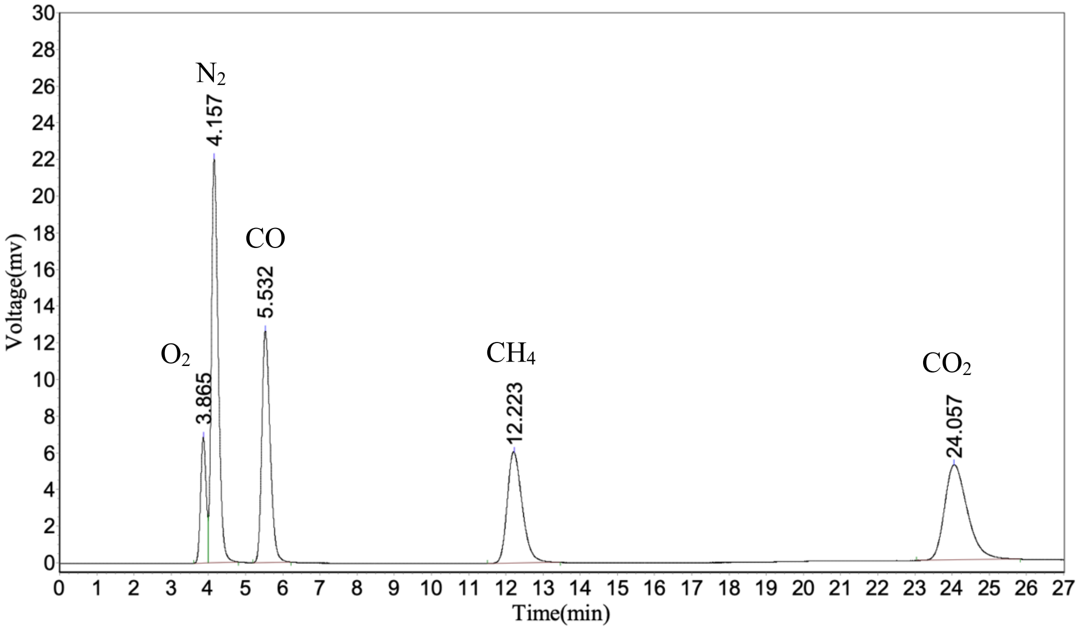

Fig. S1. GC peaks of standard gases. TCD signal with peaks of O_2, N_2, CO, CH_4, and CO_2.

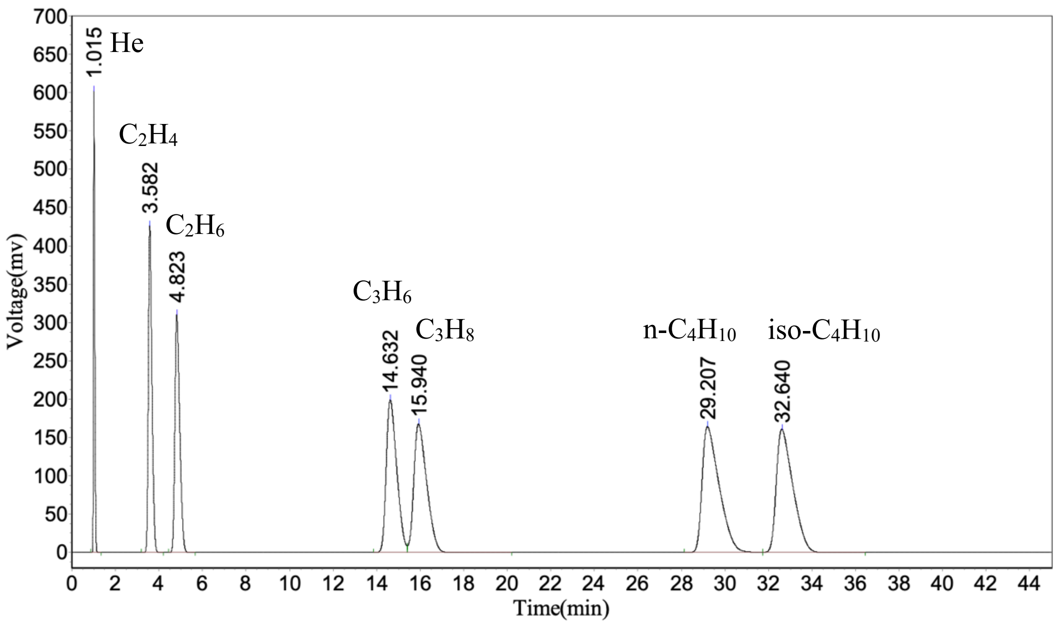

Fig. S2. GC peaks of standard gases. FID signal with peaks of He, C_2H_4, C_2H_6, C_3H_6, C_3H_8, n-C_4H_{10}, and iso-C_4H_{10}.

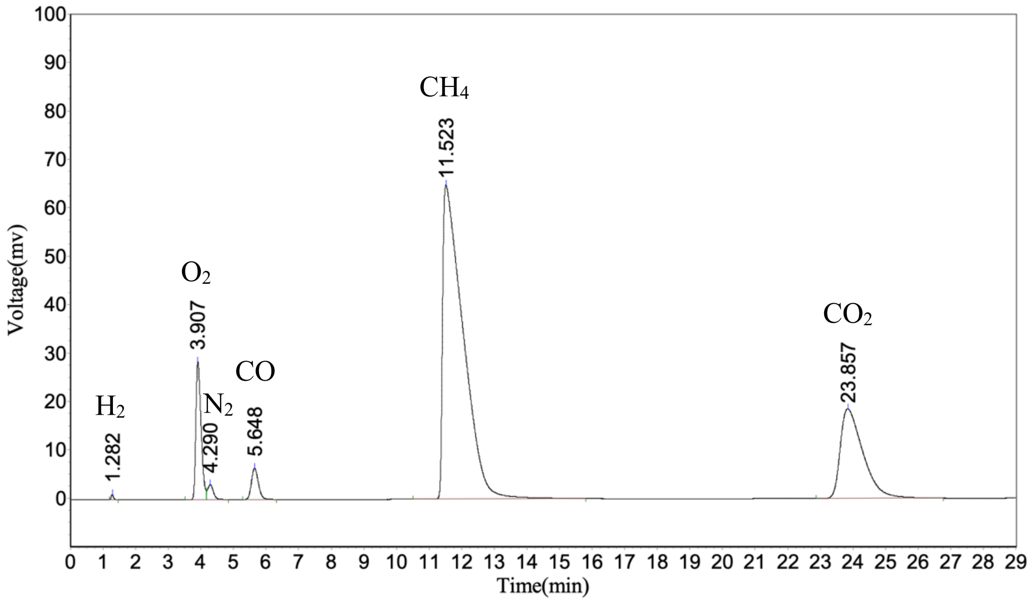

Fig. S3. Peaks of product gases with TCD signal, including H_2, O_2, N_2, CO, CH_4, and CO_2. Reaction conditions of hybrid catalyst of 5Ni/Al_2O_3 and 4.6K-20Co/Al_2O_3 at atmospheric pressure, total flow rate = 40 mL/min, reactor temperature = 490 °C, CH_4:O_2 = 2, and Ni:K-Co = 1.

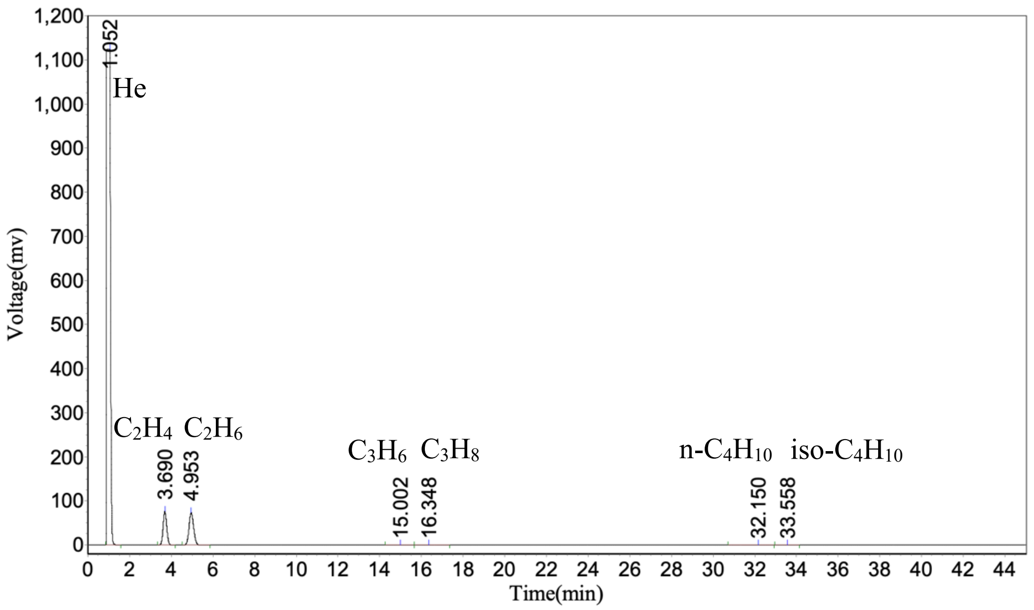

Fig. S4. Peaks of product gases with FID signal, including He, C_2H_4, C_2H_6, C_3H_6, C_3H_8, n-C_4H_{10}, and iso-C_4H_{10}. Reaction conditions of hybrid catalyst of 5Ni/Al_2O_3 and 4.6K-20Co/Al_2O_3 at atmospheric pressure, total flow rate = 40 mL/min, reactor temperature = 490 °C, CH_4:O_2 = 2, and Ni:K-Co = 1.

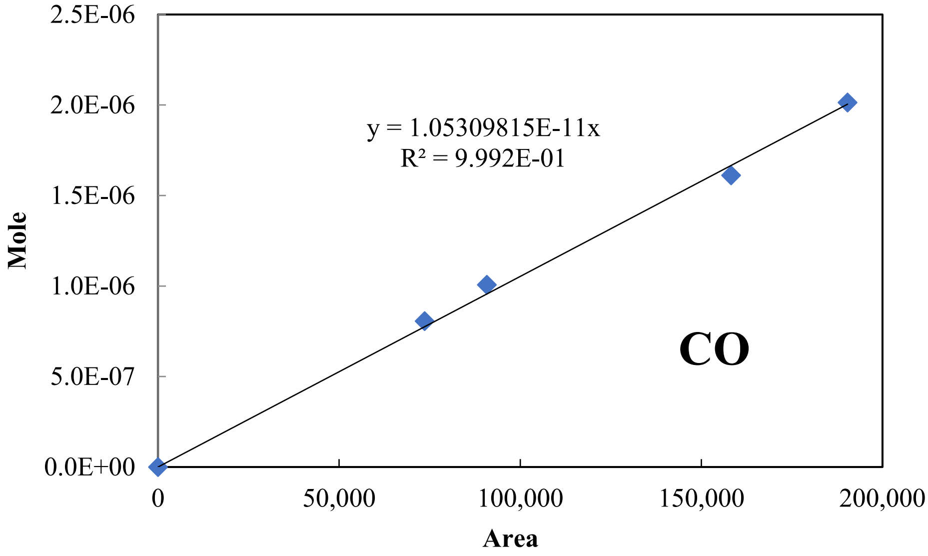

Fig. S5. Calibration curve of carbon monoxide (CO).

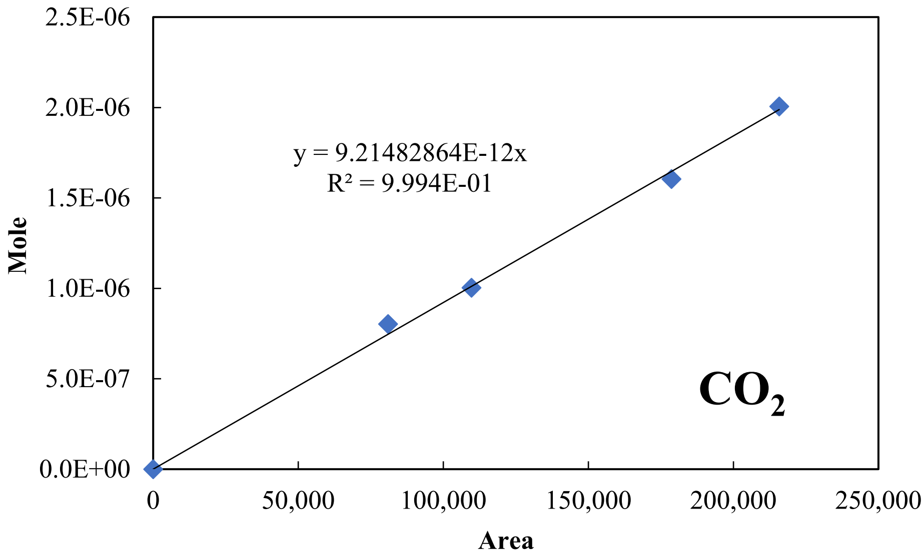

Fig. S6. Calibration curve of carbon dioxide (CO_2).

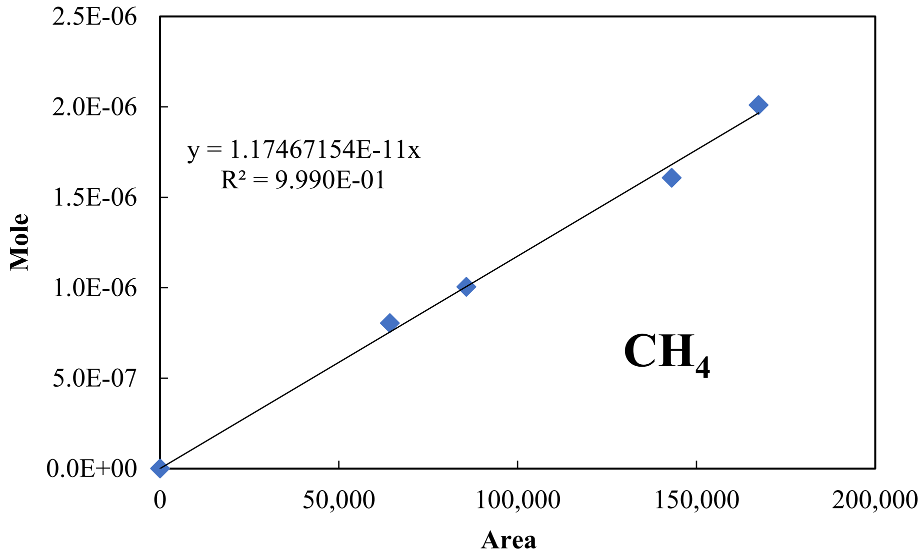

Fig. S7. Calibration curve of methane (CH_4).

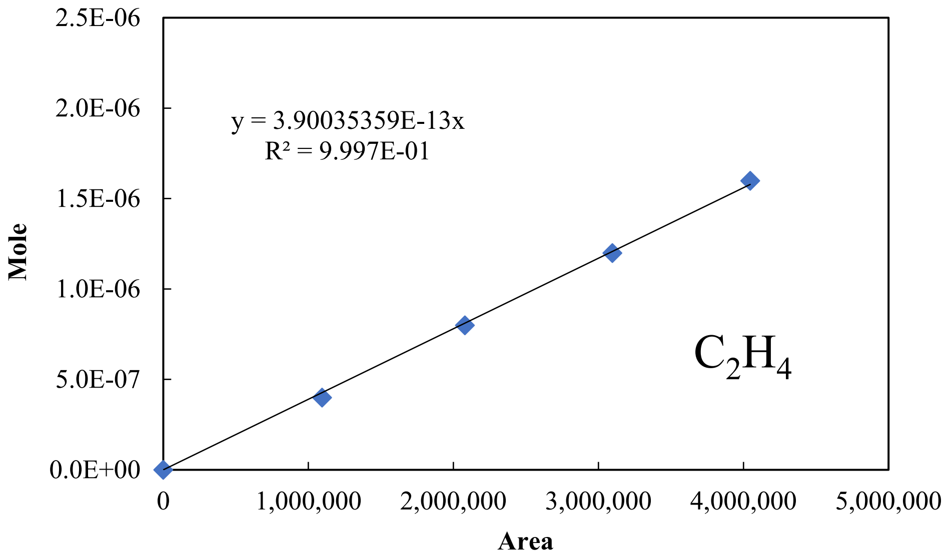

Fig. S8. Calibration curve of ethylene (C_2H_4).

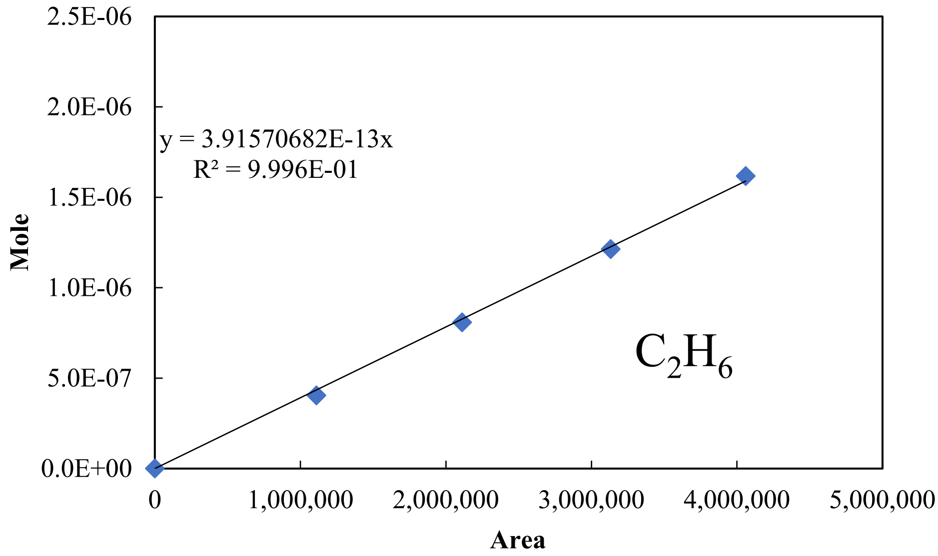

Fig. S9. Calibration curve of ethane (C_2H_6).

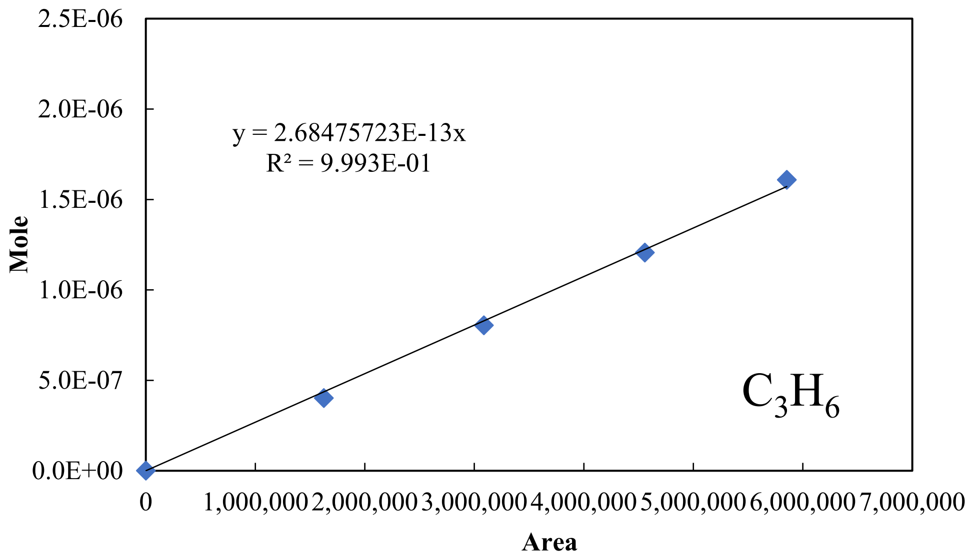

Fig. S10.1 Calibration curve of propene (C_3H_6).

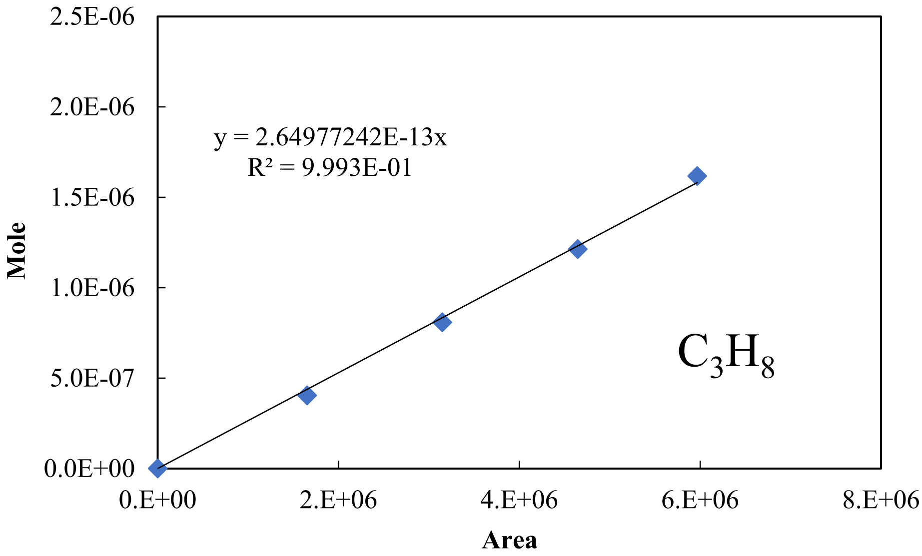

Fig. S11. Calibration curve of propane (C_3H_8).

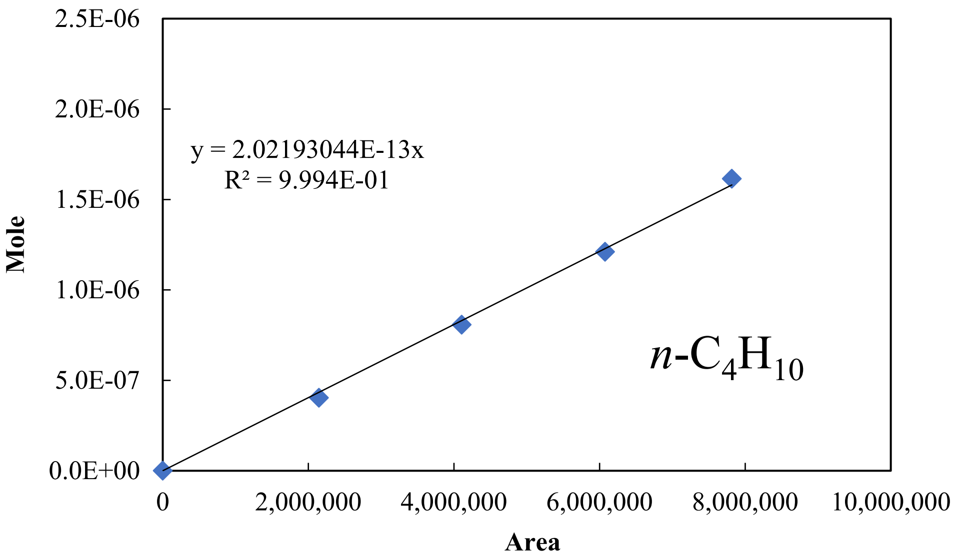

Fig. S12. Calibration curve of n-butane (n-C_4H_{10}).

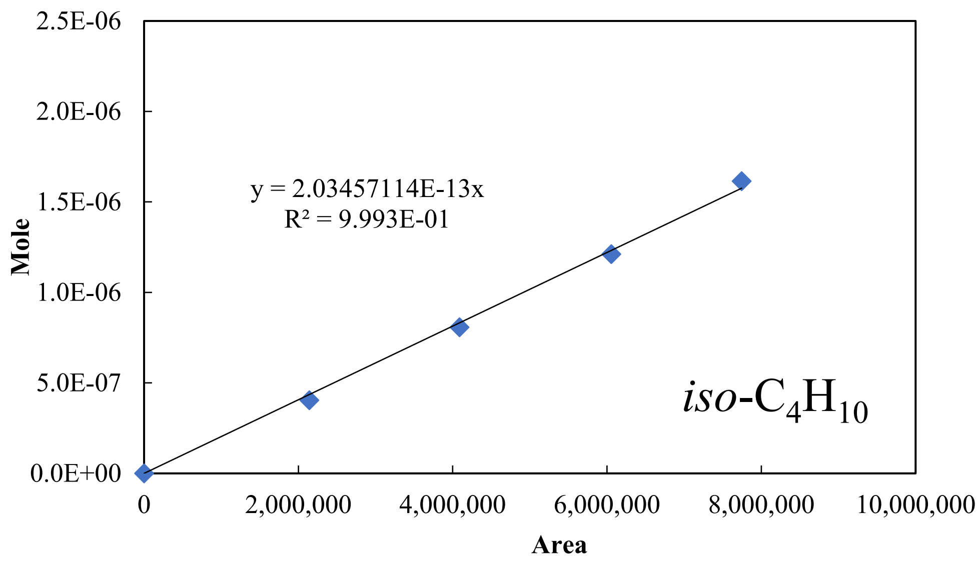

Fig. S13. Calibration curve of iso-butane (C_4H_{10}).

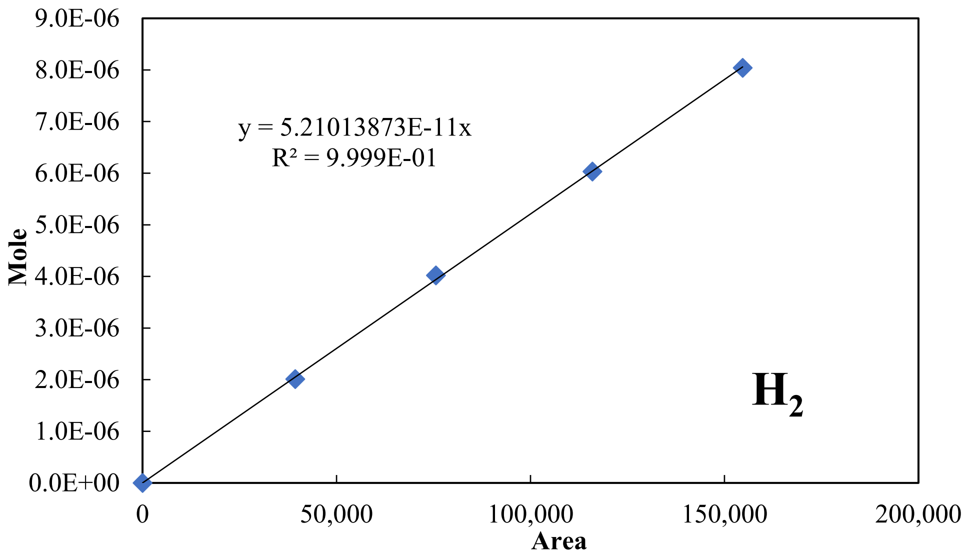

Fig. S14. Calibration curve of hydrogen (H_2).

Table S2 An example of the carbon balance for of hybrid catalyst of $5Ni/Al_2O_3$ and $4.6K\text{-}20Co/Al_2O_3$ that is shown in Fig. 13.

Time (h)	Blank CH_4 or $CH_{4,In}$ ($\times10^{-5}$) (moles)	Gases out (moles)									Gases out: Product in terms of CH_4 consumed (moles)									$CH_{4,In}$ ($\times10^{-5}$) (moles)	[a] Sum of Carbon $_{Out}$ ($\times10^{-5}$) (moles)	[b] CH_4 balance error (%)
		CO ($\times10^{-7}$)	CH_4 ($\times10^{-5}$)	CO_2 ($\times10^{-6}$)	C_2H_4 ($\times10^{-7}$)	C_2H_6 ($\times10^{-7}$)	C_3H_6 ($\times10^{-9}$)	C_3H_8 ($\times10^{-9}$)	$n\text{-}C_4H_{10}$ ($\times10^{-10}$)	$iso\text{-}C_4H_{10}$ ($\times10^{-11}$)	CO ($\times10^{-7}$)	CH_4 ($\times10^{-5}$)	CO_2 ($\times10^{-6}$)	$2*C_2H_4$ ($\times10^{-7}$)	$2*C_2H_6$ ($\times10^{-6}$)	$3*C_3H_6$ ($\times10^{-8}$)	$3*C_3H_8$ ($\times10^{-8}$)	$4*n\text{-}C_4H_{10}$ ($\times10^{-9}$)	$4*iso\text{-}C_4H_{10}$ ($\times10^{-10}$)			
1	4.80	5.45	3.54	9.99	3.70	5.48	3.73	7.09	4.61	0.97	5.45	3.54	9.99	7.39	1.10	1.12	2.13	1.84	3.90	4.80	4.78	0.32
2	4.80	6.76	3.58	9.74	3.63	5.29	3.88	6.78	0.00	0.00	6.76	3.58	9.74	7.26	1.06	1.16	2.04	0.00	0.00	4.80	4.80	-0.14
3	4.80	7.43	3.59	9.48	3.67	5.25	4.44	7.27	5.85	1.06	7.43	3.59	9.48	7.33	1.05	1.33	2.18	2.34	4.24	4.80	4.80	0.03
4	4.80	7.95	3.56	9.49	3.80	5.25	4.43	7.06	0.00	0.00	7.95	3.56	9.49	7.60	1.05	1.33	2.12	0.00	0.00	4.80	4.77	0.56
5	4.80	8.44	3.56	9.39	3.84	5.23	4.98	7.48	6.71	1.06	8.44	3.56	9.39	7.68	1.05	1.49	2.24	2.68	4.25	4.80	4.77	0.64
6	4.80	8.73	3.57	9.33	3.91	5.20	5.09	7.49	6.80	1.09	8.73	3.57	9.33	7.83	1.04	1.53	2.25	2.72	4.35	4.80	4.77	0.52
7	4.80	8.97	3.56	9.17	3.88	5.13	5.13	7.46	0.00	0.00	8.97	3.56	9.17	7.77	1.03	1.54	2.24	0.00	0.00	4.80	4.75	0.94
8	4.80	9.18	3.57	9.11	3.91	5.10	7.59	7.51	7.07	1.32	9.18	3.57	9.11	7.83	1.02	2.28	2.25	2.83	5.29	4.80	4.76	0.83
9	4.80	9.32	3.57	9.01	3.90	5.03	5.23	7.37	7.41	1.46	9.32	3.57	9.01	7.80	1.01	1.57	2.21	2.97	5.84	4.80	4.75	1.04
10	4.80	9.56	3.56	8.88	3.86	4.95	5.27	7.39	7.13	1.31	9.56	3.56	8.88	7.73	0.99	1.58	2.22	2.85	5.23	4.80	4.73	1.45
11	4.80	9.73	3.57	8.82	3.84	4.88	5.24	7.30	0.00	0.00	9.73	3.57	8.82	7.67	0.98	1.57	2.19	0.00	0.00	4.80	4.73	1.36
12	4.80	9.94	3.58	8.79	3.84	4.84	5.24	7.25	7.36	1.27	9.94	3.58	8.79	7.68	0.97	1.57	2.17	2.95	5.07	4.80	4.74	1.27
13	4.80	10.14	3.58	8.69	3.83	4.79	5.31	7.25	7.84	1.55	10.14	3.58	8.69	7.66	0.96	1.59	2.17	3.14	6.19	4.80	4.72	1.54
14	4.80	10.33	3.58	8.76	3.85	4.77	5.53	7.31	2.59	1.61	10.33	3.58	8.76	7.71	0.95	1.66	2.19	1.03	6.46	4.80	4.73	1.33
15	4.80	10.45	3.62	8.62	3.71	4.63	5.16	7.06	0.00	0.00	10.45	3.62	8.62	7.42	0.93	1.55	2.12	0.00	0.00	4.80	4.75	0.94
16	4.80	10.55	3.61	8.51	3.61	4.52	5.06	6.90	7.02	1.16	10.55	3.61	8.51	7.21	0.90	1.52	2.07	2.81	4.64	4.80	4.74	1.26
17	4.80	10.62	3.61	8.50	3.59	4.49	5.05	6.83	0.00	0.00	10.62	3.61	8.50	7.18	0.90	1.52	2.05	0.00	0.00	4.80	4.73	1.34
18	4.80	10.75	3.59	8.42	3.52	4.41	4.93	6.72	7.07	1.03	10.75	3.59	8.42	7.04	0.88	1.48	2.01	2.83	4.13	4.80	4.70	2.00
19	4.80	10.86	3.62	8.35	3.52	4.38	4.98	6.76	7.02	1.22	10.86	3.62	8.35	7.04	0.88	1.49	2.03	2.81	4.86	4.80	4.72	1.59
20	4.80	10.97	3.59	8.29	3.50	4.34	4.96	6.67	7.10	1.29	10.97	3.59	8.29	6.99	0.87	1.49	2.00	2.84	5.15	4.80	4.69	2.22
21	4.80	11.08	3.57	8.22	3.49	4.31	4.91	6.61	7.14	1.24	11.08	3.57	8.22	6.98	0.86	1.47	1.98	2.86	4.95	4.80	4.66	2.85
22	4.80	11.12	3.55	8.04	3.44	4.23	4.83	6.46	7.22	1.20	11.12	3.55	8.04	6.88	0.85	1.45	1.94	2.89	4.78	4.80	4.63	3.56
23	4.80	11.23	3.55	8.19	3.61	4.35	5.18	6.72	7.98	1.43	11.23	3.55	8.19	7.23	0.87	1.55	2.02	3.19	5.72	4.80	4.64	3.27
24	4.80	11.53	3.58	8.46	3.87	4.53	5.65	7.03	8.92	1.45	11.53	3.58	8.46	7.74	0.91	1.69	2.11	3.57	5.79	4.80	4.71	1.77

[a] Sum of carbon$_{out}$ $= 2\left(n_{C_2H_4} + n_{C_2H_6}\right) + 3\left(n_{C_3H_6} + n_{C_3H_8}\right) + 4\left(n_{C_4H_{10}}\right) + n_{CO} + n_{CO_2} + n_{CH_4,out}$

[b] CH_4 balance error (%) $= \left[n_{CH_4,in} - (\text{Sum of carbon}_{out})\right] \times 100 / n_{CH_4,in}$; where n = number of moles

Table S3 Crystalline XRD values (2θ) observed in different catalysts.

Catalyst	Crystalline phase	2θ (degree)	ICDD No.
5Ni/Al_2O_3	NiO	37.18, 43.18, 62.84, 75.56	00-047-1049
	γ-Al_2O_3	19.42, 32.73, 37.18, 39.37, 45.57, 60.60, 66.85	01-077-0396
20Co/Al_2O_3	Guite (Co_3O_4)	18.98, 31.25, 36.86, 38.51, 44.80, 55.62, 59.41, 65.30, 77.50, 78.40	00-043-1003
	γ-Al_2O_3	19.42, 32.73, 37.18, 39.37, 45.57, 60.60, 66.85	01-077-0396
4.6K-20Co/Al_2O_3	Guite (Co_3O_4)	18.97, 31.25, 36.84, 38.57, 44.80, 55.65, 59.35, 65.29, 77.51, 78.55	00-043-1003
	Niter (KNO_3)	23.51, 23.76, 29.39, 32.30, 33.78, 41.13, 41.72, 46.47, 64.76	01-071-1558
	γ-Al_2O_3	19.42, 32.73, 37.18, 39.37, 45.57, 60.60, 66.85	01-077-0396
Spent 5Ni/Al_2O_3	NiO	37.14, 43.18, 62.80, 75.36	00-047-1049
	γ-Al_2O_3	19.42, 32.73, 37.18, 39.37, 45.57, 60.60, 66.85	01-077-0396
Spent 4.6K-20Co/Al_2O_3	Guite (Co_3O_4)	18.96, 31.22, 36.80, 38.52, 44.80, 55.60, 59.31, 65.20, 77.37, 77.98	00-043-1003
	Niter (KNO_3)	23.51, 23.76, 29.39, 32.30, 33.78, 41.13, 41.72, 46.47, 64.76	01-071-1558
	γ-Al_2O_3	19.42, 32.73, 37.18, 39.37, 45.57, 60.60, 66.85	01-077-0396

Table S4 EDX analysis of each prepared catalyst.

<table>
<tr><th rowspan="2">Catalyst</th><th colspan="5">EDX and weight percent elemental</th></tr>
<tr><th>Ni</th><th>O</th><th>Al</th><th>Co</th><th>K</th></tr>
<tr><td>5Ni/ Al_2O_3</td><td>
</td><td>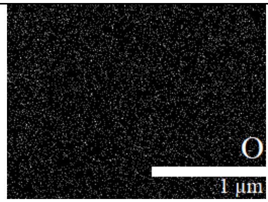
</td><td>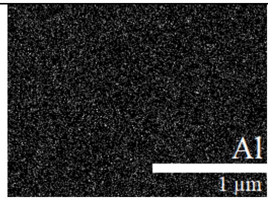
</td><td></td><td></td></tr>
<tr><td>20Co/ Al_2O_3</td><td></td><td>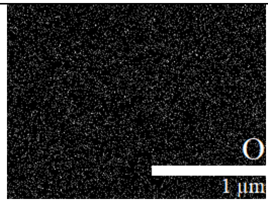
</td><td>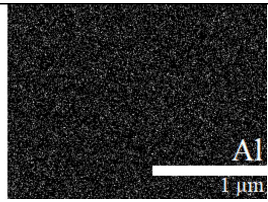
</td><td>
</td><td></td></tr>
<tr><td>4.6K-20Co/ Al_2O_3</td><td></td><td>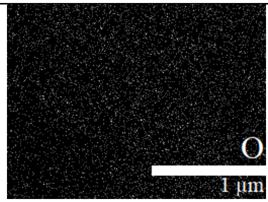
</td><td>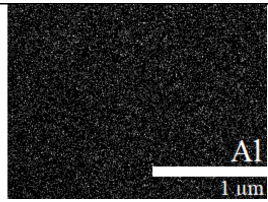
</td><td>
</td><td>
</td></tr>
</table>

Table S5 A review of the OCM catalysts reported in the literature.

Catalyst	Reaction temperature (˚C)	C_{2+} yield (%)	C_{2+} selectivity (%)	CH_4 conversion (%)	Ref.
Ni/Al_2O_3 and $K-Co/Al_2O_3$ (Hybrid catalyst)	490	4.30	15.80	27.19	This work
Na_2WO_4/SiO_2	800	9.1	74.3	12.3	[1]
$Mn-Na_2WO_4/SiO_2$	800	23.9	64.9	36.8	[1]
$Mn/Na_2WO_4/SiO_2$	850	26.4	80.0	33.0	[2]
Na_2WO_4/SiO_2	850	22.9	52.0	44.0	[2]
Na_2WO_4/SiO_2	775	7.0	63.0	11.0	[3]
$V/Na_2WO_4/SiO_2$	775	1.2	12.0	10.0	[3]
$Cr/Na_2WO_4/SiO_2$	775	2.4	24.0	10.0	[3]
$Mn/Na_2WO_4/SiO_2$	775	16.0	80.0	20.0	[3]
$Fe/Na_2WO_4/SiO_2$	775	9.0	60.0	15.0	[3]
$CO/Na_2WO_4/SiO_2$	775	11.0	68.0	16.0	[3]
$Zn/Na_2WO_4/SiO_2$	775	6.0	63.0	9.0	[3]
$Mn-Na_2WO_4/SiO_2$	850	17.0	75.0	22.0	[4]
$Na_2WO_4/Mn/SiO_2$	850	17.2	54.0	32.0	[5]
$W-Mn/SiO_2$	820	20.7	68.4	30.3	[6]
$W-Li/SiO_2$	800	6.0	52.0	10.0	[7]
$Mn-Li/SiO_2$	800	6.0	40.0	15.0	[7]
$Mn-W/SiO_2$	800	6.0	40.0	15.0	[7]
$Mn-0.1Li-W/SiO_2$	800	11.0	58.0	18.0	[7]
$Mn-0.25Li-W/SiO_2$	800	15.0	78.0	18.0	[7]
$W-Li-W/SiO_2$	800	15.0	79.0	19.0	[7]
$Na_2WO_4/Mn/SiO_2$	800	11.2	27.4	41.0	[8]
$La/Na_2WO_4/Mn/SiO_2$	800	10.6	25.4	41.7	[8]
$Na-W-Mn/SiO_2$	850	29.0	69.0	42.0	[9]
Na_2WO_4/SiO_2	800	15.0	74.0	20.0	[10]
W/SiO_2	800	6.0	54.0	11.0	[10]
Mn/SiO_2	800	9.0	43.0	19.0	[10]
$W-Na-Mn/SiO_2$	775	18.3	39.6	46.1	[11]
$Mo-Na-Mn/SiO_2$	775	12.5	37.2	33.6	[11]
$Nb-Na-Mn/SiO_2$	775	13.0	33.2	39.3	[11]
$V-Na-Mn/SiO_2$	775	2.7	8.0	33.5	[11]
$Cr-Na-Mn/SiO_2$	775	4.6	11.5	40.1	[11]
$Ce-Mn/Na_2WO_4/SiO_2$	840	21.1	62.4	33.9	[12]
$Na-W-Mn/SiO_2$	800	19.1	63.2	30.2	[13]
$Mn-Na_2WO_4/SiO_2$	825	19.1	72.2	26.5	[14]
Mn/SiO_2	800	0.6	14.4	5.7	[15]
Na_2WO_4/SiO_2	800	2.9	69.0	4.8	[15]
$Mn-Na_2WO_4/SiO_2$	800	18.5	73.3	28.5	[15]
$NaCl-Mn-Na_2WO_4/SiO_2$	750	34.6	62.9	55.0	[16]

Table S5 A review of the OCM catalysts reported in the literature. (continued)

Catalyst	Reaction temperature (˚C)	C_{2+} yield (%)	C_{2+} selectivity (%)	CH_4 conversion (%)	Ref.
KCl-Mn-Na_2WO_4/SiO_2	750	27.0	75.3	35.9	[16]
CsCl-Mn-Na_2WO_4/SiO_2	750	22.6	74.9	30.1	[16]
LiCl-Mn-Na_2WO_4/SiO_2	750	11.3	80.2	14.1	[16]
Mn-Na_2WO_4/SiO_2	750	5.2	63.4	8.2	[16]
Mn_xO_y-Na_2WO_4/D11-10	750	3.6	52.9	6.7	[17]
Mn_xO_y-Na_2WO_4/SiO_2 (grade 923)	750	1.3	63.6	2.0	[17]
Mn_xO_y-Na_2WO_4/SiO_2 (fumed)	750	4.5	61.3	7.4	[17]
Mn_xO_y-Na_2WO_4/Aerosil TT 600	750	4.5	60.7	7.3	[17]
Mn_xO_y-Na_2WO_4/Aeroperl R 806/30	750	4.9	68.9	7.1	[17]
Mn_xO_y-Na_2WO_4/Aerosil OX 50	750	3.5	55.4	6.4	[17]
Mn_xO_y-Na_2WO_4/Aerosil 380	750	4.2	62.6	6.6	[17]
Mn_xO_y-Na_2WO_4/Aerosil 300	750	3.3	57.4	5.9	[17]
Mn_xO_y-Na_2WO_4/Sipernat D10	750	3.5	80.3	4.4	[17]
Mn_xO_y-Na_2WO_4/Sipernat 310	750	5.4	75.8	7.0	[17]
Mn_xO_y-Na_2WO_4/SBA-15	750	10.4	73.4	14.1	[17]
Na_2WO_4/Mn/SiO_2	800	2.5	67.6	3.2	[18]
Na_2WO_4-Mn/SiO_2	800	19.6	66.4	29.5	[18]
TiO_2-Mn_2O_3-Na_2WO_4/SiO_2	700	14.0	70.0	20.0	[19]
TiO_2-Mn_2O_3-Na_2WO_4/SiO_2	720	19.7	76.0	26.0	[20]
Mn_2O_3-TiO_2-Na_2WO_4/SiO_2	650	13.6	62.0	22.0	[20]
Na_2WO_4/Mn/SiO_2 (silica gel)	775	16.9	50.8	33.4	[21]
Na_2WO_4/Mn/SiO_2 (silica gel)	800	17.1	51.0	33.5	[21]
Na_2WO_4/Mn/SiO_2 (fumed silica)	800	16.5	52.7	33.3	[21]
Mn/Na_2WO_4/SiO_2	725	16.0	79.8	20.2	[22]
Mn-Na-W/SiO_2	750	16.0	64.0	25.0	[23]
Al-Na_2WO_4/SiO_2	800	3.2	37.0	7.69	[24]
Li-Na_2WO_4/SiO_2	800	4.6	47.8	9.56	[24]
La-Na_2WO_4/SiO_2	800	6.1	49.5	11.9	[24]
Cu-Na_2WO_4/SiO_2	800	7.5	22.3	33.8	[24]
Cr-Na_2WO_4/SiO_2	800	9.8	29.9	27.7	[24]
Na_2-WO_4/SiO_2	800	10.9	24.0	33.5	[24]
Mg-Na_2WO_4/SiO_2	800	12.5	53.2	21.6	[24]
Ni-Na_2WO_4/SiO_2	800	13.7	36.1	35.4	[24]
Ce-Na_2WO_4/SiO_2	800	15.4	32.9	42.1	[24]
Zn-Na_2WO_4/SiO_2	800	17.8	65.9	25.5	[24]
Co-Na_2WO_4/SiO_2	800	18.4	10.2	41.8	[24]

Table S5 A review of the OCM catalysts reported in the literature. (continued)

Catalyst	Reaction temperature (˚C)	C_{2+} yield (%)	C_{2+} selectivity (%)	CH_4 conversion (%)	Ref.
Mn-W/SiO_2	800	11.0	48.0	24.0	[24]

Ce-W/SiO_2	800	7.0	35.0	20.0	[24]
Mn-Na/SiO_2	800	14.0	44.0	31.0	[24]
Na_2WO_4-Mn/SiO_2	800	20.0	67.0	30.0	[24]
Na_2WO_4-Ce/SiO_2	800	20.0	74.0	27.0	[24]
TiO_2-Mn_2O_3-Na_2WO_4/SiO_2	700	16.7	73.0	23.0	[25]
Na_2WO_4-TiO_2/SiO_2	700	4.9	71.7	6.8	[26]
MnO_x-Na_2WO_4/SiO_2	770	12.4	70.4	17.6	[27]
Nb-MnO_x-Na_2WO_4/SiO_2	770	15.2	68.2	22.3	[27]
Ti-MnO_x-Na_2WO_4/SiO_2	770	11.2	70.4	15.9	[27]
Sn-MnO_x-Na_2WO_4/SiO_2	770	7.5	69.5	10.8	[27]
Ce-MnO_x-Na_2WO_4/SiO_2	770	12.7	66.7	19.0	[27]
Fe-MnO_x-Na_2WO_4/SiO_2	770	15.8	65.5	24.1	[27]
Ge-MnO_x-Na_2WO_4/SiO_2	770	16.4	70.7	23.2	[27]
Mn_2O_3-Na_2WO_4/SiC	800	20.5	54.5	37.5	[28]
Mn_2O_3-Na_2WO_4/SiO_2	700	23.5	60.5	39.7	[29]
Na_2WO_4-Ti-Mn/SiO_2	700	22.1	62.3	35.4	[30]
Na_2WO_4-TiO_2-MnO_x-$Sr_{0.25}$/SiO_2	750	22.9	62.5	36.6	[31]
$(NH_4)_2WO_4$/SiO_2	850	2.4	20	12	[32]
Mn/SiO_2	850	5.29	23	23	[32]
Mn/Na_2WO_4/SiO_2	850	8	40	20	[32]
Sn-W-Mn/SiO_2	750	20.22	68.1	29.7	[32]
Ce-Na_2WO_4/ TiO_2	800	26.2	52.3	50.1	[33]
La-Li-Mn/WO_3/TiO_2	750	19.2	64	30	[34]
Mn-Na_2WO_4/CeO_2-TiO_2	775	30.3	52.8	57.4	[35]
Ce-Mn/Na_2WO_4/SiO_2	840	16.24	65.5	24.8	[12]
S-Na-W-Mn-Zr/SiO_2	750	16.18	42.7	37.9	[36]
S-Na-W-Mn-Zr/SiO_2	750	16.3	46.2	35.3	[37]
Na_2WO_4-Mn/SiO_2	850	11.18	51.9	21.5	[38]
Na_2WO_4-Mn/SBA-15	850	14.78	56.2	26.3	[32]
$MnTiO_3$-Na_2WO_4/SBA-15	750	8.84	68	13	[39]
Mn_xO_y-Na_2WO_4/TiO_2-rutile	700	24.82	63	39.4	[40]
Mn_2O_3-Na_2WO_4/TiO_2-SiO_2	750	2.91	42.8	6.8	[19]
SiO_2@MnO_x@Na_2WO_4@SiO_2	700	17.76	74	24	[32]

References:

[1] Z. C. Jiang, C.-J. Yu, X.-P. Fang, S.-B. Li, H.-L. Wang, Oxide/support interaction and surface reconstruction in the sodium tungstate (Na_2WO_4)/silica system, Journal of Physical Chemistry A, 97 (1993) 12870-12875.

[2] A. Palermo, J.P.H. Vazquez, M.S. Tikhov, R.M. Lambert, Critical influence of the amorphous silica-to-cristobalite phase transition on the performance of Mn/Na_2WO_4/SiO_2 catalysts for the oxidative coupling of methane, Journal of Catalysis, 177 (1998) 259-266.

[3] A. Malekzadeh, A. Khodadadi, M. Abedini, M. Amini, A. Bahramian, A.K. Dalai, Correlation of electrical properties and performance of OCM MO_x/Na_2WO_4/SiO_2 catalysts, Catalysis Communications, 2 (2001) 241-247.

[4] S.-F. Ji, T.-C. Xiao, S.-B. Li, C.-Z. Xu, R.-L. Hou, K.S. Coleman, M.L.H. Green, The relationship between the structure and the performance of Na-W-Mn/SiO_2 catalysts for the oxidative coupling of methane, Applied Catalysis A: General, 225 (2002) 271-284.

[5] S. Ji, T. Xiao, S. Li, L. Chou, B. Zhang, C. Xu, R. Hou, A.P.E. York, M.L.H. Green, Surface WO_4 tetrahedron: The essence of the oxidative coupling of methane over M-W-Mn/SiO_2 catalysts, Journal of Catalysis, 220 (2003) 47-56.

[6] J. Wang, L. Chou, B. Zhang, H. Song, J. Zhao, J. Yang, S. Li, Comparative study on oxidation of methane to ethane and ethylene over Na_2WO_4-Mn/SiO_2 catalysts prepared by different methods, J Mol Catal A-Chem, 245 (2006) 272-277.

[7] A. Malekzadeh, A. Khodadadi, A.K. Dalai, M. Abedini, Oxidative coupling of methane over lithium doped (Mn+W)/SiO_2 catalysts, Journal of Natural Gas Chemistry, 16 (2007) 121-129.

[8] J. Wu, H. Zhang, S. Qin, C. Hu, La-promoted Na_2WO_4/Mn/SiO_2 catalysts for the oxidative conversion of methane simultaneously to ethylene and carbon monoxide, Applied Catalysis A: General, 323 (2007) 126-134.

[9] Y.T. Chua, A.R. Mohamed, S. Bhatia, Oxidative coupling of methane for the production of ethylene over sodium-tungsten-manganese-supported-silica catalyst (Na-W-Mn/SiO_2), Applied Catalysis A: General, 343 (2008) 142-148.

[10] Z. Gholipour, A. Malekzadeh, R. Hatami, Y. Mortazavi, A. Khodadadi, Oxidative coupling of methane over (Na_2WO_4+Mn or Ce)/SiO_2 catalysts: In situ measurement of electrical conductivity, Journal of Natural Gas Chemistry, 19 (2010) 35-42.

[11] S. Mahmoodi, M.R. Ehsani, S.M. Ghoreishi, Effect of promoter in the oxidative coupling of methane over synthesized Mn/SiO_2 nanocatalysts via incipient wetness impregnation, Journal of Industrial and Engineering Chemistry, 16 (2010) 923-928.

[12] S.M.K. Shahri, A.N. Pour, Ce-promoted Mn/Na_2WO_4/SiO_2 catalyst for oxidative coupling of methane at atmospheric pressure, Journal of Natural Gas Chemistry, 19 (2010) 47-53.

[13] J.Y. Lee, W. Jeon, J.-W. Choi, Y.-W. Suh, J.-M. Ha, D.J. Suh, Y.-K. Park, Scaled-up production of C_2 hydrocarbons by the oxidative coupling of methane over pelletized Na_2WO_4/Mn/SiO_2 catalysts: Observing hot spots for the selective process, Fuel, 106 (2013) 851-857.

[14] H.R. Godini, A. Gili, O. Görke, S. Arndt, U. Simon, A. Thomas, R. Schomäcker, G. Wozny, Sol–gel method for synthesis of Mn–Na_2WO_4/SiO_2 catalyst for methane oxidative coupling, Catalysis Today, 236 (2014) 12-22.

[15] T.W. Elkins, H.E. Hagelin-Weaver, Characterization of Mn-Na_2WO_4/SiO_2 and Mn-Na_2WO_4/MgO catalysts for the oxidative coupling of methane, Applied Catalysis A: General, 497 (2015) 96-106.

[16] N. Hiyoshi, T. Ikeda, Oxidative coupling of methane over alkali chloride-Mn-Na_2WO_4/SiO_2 catalysts: Promoting effect of molten alkali chloride, Fuel Processing Technology, 133 (2015) 29-34.

[17] M. Yildiz, Y. Aksu, U. Simon, T. Otremba, K. Kailasam, C. Göbel, F. Girgsdies, O. Görke, F. Rosowski, A. Thomas, R. Schomäcker, S. Arndt, Silica material variation for the Mn_xO_y-Na_2WO_4/SiO_2, Applied Catalysis A: General, 525 (2016) 168-179.

[18] V. Fleischer, R. Steuer, S. Parishan, R. Schomäcker, Investigation of the surface reaction network of the oxidative coupling of methane over $Na_2WO_4/Mn/SiO_2$ catalyst by temperature programmed and dynamic experiments, Journal of Catalysis, 341 (2016) 91-103.

[19] P. Wang, G. Zhao, Y. Liu, Y. Lu, TiO_2-doped Mn_2O_3-Na_2WO_4/SiO_2 catalyst for oxidative coupling of methane: Solution combustion synthesis and $MnTiO_3$-dependent low-temperature activity improvement, Applied Catalysis A: General, 544 (2017) 77-83.

[20] P. Wang, G. Zhao, Y. Wang, Y. Lu, $MnTiO_3$-driven low-temperature oxidative coupling of methane over TiO_2-doped Mn_2O_3-Na_2WO_4/SiO_2 catalyst, Science Advances, 3 (2017) e1603180.

[21] R.T. Yunarti, S. Gu, J.-W. Choi, J. Jae, D.J. Suh, J.-M. Ha, Oxidative coupling of methane using Mg/Ti-doped SiO_2-supported Na_2WO_4/Mn catalysts, ACS Sustainable Chemistry & Engineering, 5 (2017) 3667-3674.

[22] C. Uzunoglu, A. Leba, R. Yildirim, Oxidative coupling of methane over Mn-Na_2WO_4 catalyst supported by monolithic SiO_2, Applied Catalysis A: General, 547 (2017) 22-29.

[23] N.S. Hayek, N.S. Lucas, C.W. Damouny, O.M. Gazit, Critical surface parameters for the oxidative coupling of methane over the Mn-Na-W/SiO_2 catalyst, ACS Appl Mater Interfaces, 9 (2017) 40404-40411.

[24] S. Gu, H.-S. Oh, J.-W. Choi, D.J. Suh, J. Jae, J. Choi, J.-M. Ha, Effects of metal or metal oxide additives on oxidative coupling of methane using Na_2WO_4/SiO_2 catalysts: Reducibility of metal additives to manipulate the catalytic activity, Applied Catalysis A: General, 562 (2018) 114-119.

[25] P. Wang, X. Zhang, G. Zhao, Y. Liu, Y. Lu, Oxidative coupling of methane: MO_x-modified (M=Ti, Mg, Ga, Zr) Mn_2O_3-Na_2WO_4/SiO_2 catalysts and effect of MO_x modification, Chinese Journal of Catalysis, 39 (2018) 1395-1402.

[26] A. Seubsai, P. Tiencharoenwong, P. Kidamorn, C. Niamnuy, Synthesis of light hydrocarbons via oxidative coupling of methane over silica-supported Na_2WO_4-TiO_2 catalyst, Engineering Journal, 23 (2019) 169-182.

[27] N.S. Hayek, G.J. Khlief, F. Horani, O.M. Gazit, Effect of reaction conditions on the oxidative coupling of methane over doped MnO_x-Na_2WO_4/SiO_2 catalyst, Journal of Catalysis, 376 (2019) 25-31.

[28] J. Kim, L.-H. Park, J.-M. Ha, E.D. Park, Oxidative coupling of methane over Mn_2O_3-Na_2WO_4/SiC catalysts, Catalysts, 9 (2019).

[29] T. Chukeaw, S. Sringam, M. Chareonpanich, A. Seubsai, Screening of single and binary catalysts for oxidative coupling of methane to value-added chemicals, Molecular Catalysis, 470 (2019) 40-47.

[30] S. Sringam, P. Kidamorn, T. Chukeaw, M. Chareonpanich, A. Seubsai, Investigation of metal oxide additives onto Na_2WO_4-Ti/SiO_2 catalysts for oxidative coupling of methane to value-added chemicals, Catalysis Today, 358 (2020) 263-269.

[31] P. Kidamorn, W. Tiyatha, T. Chukeaw, C. Niamnuy, M. Chareonpanich, H. Sohn, A. Seubsai, Synthesis of value-added chemicals via oxidative coupling of methanes over Na_2WO_4-TiO_2-MnO_x/SiO_2 catalysts with alkali or alkali earth oxide additives, ACS Omega, 5 (2020) 13612-13620.

[32] J. Liu, J. Yue, M. Lv, F. Wang, Y. Cui, Z. Zhang, G. Xu, From fundamentals to chemical engineering on oxidative coupling of methane for ethylene production: A review, Carbon Resources Conversion, 5 (2022) 1-14.

[33] V. Jodaian, M. Mirzaei, Ce–promoted Na_2WO_4/TiO_2 catalysts for the oxidative coupling of methane, Inorganic Chemistry Communications, 100 (2019) 97-100.

[34] F. Cheng, J. Yang, L. Yan, J. Zhao, H. Zhao, H. Song, L.J. Chou, Enhancement of La2O3 to Li-Mn/WO_3/TiO_2 for oxidative coupling of methane, Journal of Rare Earths, 38 (2020) 167-174.

[35] G.J. Kim, J.T. Ausenbaugh, H.T. Hwang, Effect of TiO2 on the Performance of Mn/Na2WO4 Catalysts in Oxidative Coupling of Methane, Industrial & Engineering Chemistry Research, 60 (2021) 3914-3921.

[36] W. Zheng, D. Cheng, N. Zhu, F. Chen, X. Zhan, Studies on the structure and catalytic performance of S and P promoted Na-W-Mn-Zr/SiO_2 catalyst for oxidative coupling of methane, Journal of Natural Gas Chemistry, 19 (2010) 15-20.

[37] W. Zheng, D. Cheng, F. Chen, X. Zhan, Characterization and catalytic behavior of Na-W-Mn-Zr-S-P/SiO_2 prepared by different methods in oxidative coupling of methane, Journal of Natural Gas Chemistry, 19 (2010) 515-521.

[38] H. Liu, D. Yang, R. Gao, L. Chen, S. Zhang, X. Wang, A novel Na_2WO_4–Mn/SiC monolithic foam catalyst with improved thermal properties for the oxidative coupling of methane, Catalysis Communications, 9 (2008) 1302-1306.

[39] T. Chukeaw, W. Tiyatha, K. Jaroenpanon, T. Witoon, P. Kongkachuichay, M. Chareonpanich, K. Faungnawakij, N. Yigit, G. Rupprechter, A. Seubsai, Synthesis of value-added hydrocarbons via oxidative coupling of methane over $MnTiO_3$-Na_2WO_4/SBA-15 catalysts, Process Safety and Environmental Protection, 148 (2021) 1110-1122.

[40] M. Yıldız, Mesoporous TiO_2-rutile supported Mn_xO_y-Na_2WO_4: Preparation, characterization and catalytic performance in the oxidative coupling of methane, Journal of Industrial and Engineering Chemistry, 76 (2019) 488-499.